Journal of Catalysis **208,** 422–434 (2002)
doi:10.1006/jcat.2002.3594

Vanadium Oxide Overlayers on Rhodium: Influence of the Reduction Temperature on the Composition and on the Promoting Effect in CO Hydrogenation

Wolfgang Reichl and Konrad Hayek[1]

Institut für Physikalische Chemie, Leopold-Franzens-Universität Innsbruck, Innrain 52a, A-6020 Innsbruck, Austria

Received December 10, 2001; revised February 26, 2002; accepted February 26, 2002

Vanadia adlayers on a Rh surface promote the hydrogenation of CO. This promotion was investigated with particular emphasis on the effect of the oxidation state of vanadium. Inverse model catalysts were prepared by UHV deposition of submonolayer amounts of metallic vanadium on a Rh foil in an oxygen atmosphere. After oxidation at 673 K the catalyst was reduced in hydrogen under specified conditions and the surface composition was determined by Auger electron spectroscopy. The kinetics of the reaction were then measured at 573 K and atmospheric pressure. The reaction rate is always increased with respect to the bare Rh surface but depends strongly on the reduction temperature. After reduction up to 673 K the observed rate increase can be correlated to the existence of two VO_x adlayer phases of different oxygen content. Enhanced CO dissociation at the perimeter sites of the VO_x islands leads to enhanced initial hydrogenation rates but also to enhanced deactivation of the catalyst. Raising the reduction temperature above 773 K results in the formation of metallic V, which is partially dissolved in the bulk, resulting in a V/Rh subsurface alloy with a Rh-terminated surface. This surface is particularly active for CO hydrogenation and less susceptible to deactivation by carbon deposition.

Key Words: **CO hydrogenation; vanadium oxide; V/Rh subsurface alloy; model catalyst; metal-support interaction.**

1. INTRODUCTION

Reducible transition metal oxides like titania, ceria, and vanadia have a strong effect on the catalytic properties of group VIII metals which can be promoting or inhibiting, depending on the reaction type and on the valence state of the transition metal. High-temperature reduction (>773 K) usually transforms the system into the "SMSI" state, characterised by a strong decrease in the CO and hydrogen chemisorption capacity and a decreased activity for skeletal hydrocarbon reactions (1). Some of the observed phenomena can be explained by a partial decoration of the noble metal surface by substoichiometric oxide layers, as revealed in model studies on noble metal–titania systems (2–6). Blocking of metal sites by migrating overlayers must be taken into account whenever mobile suboxides are formed upon reduction. No evidence of decorating layers has been obtained after reduction of ceria-supported noble metals under comparable conditions, which has led to the conclusion that the inhibiting effects observed on ceria and other refractory oxides are merely "electronic" (7).

On the other hand, certain reactions will benefit from the interaction between metal particles and supporting oxide due to an increased number of noble metal–oxide interface sites with high reaction probability. For instance, the CO hydrogenation on noble metal particles is generally promoted by transition metal oxides (8), and likewise by deposition of oxide submonolayers on a noble metal surface (9). In a number of studies Somorjai and coworkers (10–14) investigated this reaction on polycrystalline Rh surfaces partly covered with different reducible oxides. They concluded that mainly sites at the perimeter of the two-dimensional oxide islands are involved in the promotion. Although the importance of these sites is generally recognised, the origin of the promotion is not completely clear. Boffa *et al.* (14) observed a connection between the promotional effect and the Lewis acidity of the oxide in its highest valence state.

However, one must anticipate that the interaction is determined by the *actual* valence state of the transition metal during the reaction. The morphology and composition of reducible oxides are very sensitive to the experimental conditions during deposition (e.g., oxygen partial pressure and temperature). Furthermore, restructuring usually occurs during annealing and oxidation–reduction procedures applied for catalyst activation and regeneration. Vanadium oxides tend to change structure and composition very easily. This has also been verified in a number of studies of VO_x deposits on metal surfaces (10, 13, 15). In recent STM and LEED studies Surnev and coworkers (16–19) observed that on Pd(111) a variety of surface structures of ultrathin vanadium oxide films are formed at varying coverage and temperature. The stoichiometry and morphology of the

[1] To whom correspondence should be addressed. Fax: +43 512 507 2925. E-mail: konrad.hayek@uibk.ac.at.

0021-9517/02 $35.00

low-coverage 2D phases depends on the preparation conditions. Over a wide range of temperature and composition a surface V_2O_3 layer is the energetically most stable configuration (18, 19). Upon high-temperature annealing these vanadium oxide layers decompose and are converted to island structures of a V/Pd subsurface alloy with a palladium-terminated surface. There are many indications that layers of vanadium oxide resp. vanadium metal will behave similarly on palladium and on rhodium surfaces (20–23).

The following questions now arise: Is it possible to quantify an effect of the reduction temperature on the catalytic activity of a vanadium oxide-covered rhodium surface, and if so, is it related to chemical or structural properties of the overlayer? Furthermore, how does the transition from the oxide surface to the reduced (probably Rh terminated) surface affect the catalytic activity?

Previously we could show that the promotion of the reaction on a vanadia-modified rhodium surface depends on the temperature of prereduction with hydrogen (20). In order to provide a more detailed answer to the above questions we performed a quantitative study on the influence of hydrogen reduction on the composition of vanadium oxide deposits on rhodium and on its effect on the CO hydrogenation. Following the classical approach by the Somorjai group, "inverse" model catalysts have been prepared by UHV deposition of vanadium on a polycrystalline substrate in an oxygen atmosphere. The submonolayer coverage range, with bare Rh and vanadium oxide patches coexisting on the surface, is best suited to study metal–oxide interactions. Oxidative and reductive treatments (temperature range between 300 and 1200 K and pressure range from 10^{-7} to 200 mbar) were applied to the samples prior to reaction. Changes in the surface composition were determined by AES and the catalytic activity was measured *in situ* under exceptionally "clean" conditions (24). As indicated, the properties of VO_x overlayers on rhodium and palladium surfaces will be quite similar. The results were therefore related to those for the Pd(111) surface obtained by Surnev and coworkers (16–19).

2. EXPERIMENTAL

The experiments were performed in an ultrahigh vacuum system combined with a high-pressure reaction cell (HPC) described in detail in (24). This experimental setup consists of a conventional UHV chamber with a long travel z-manipulator and a small-volume Pyrex glass reactor (60 ml) attached to the UHV chamber via a sample transfer port. The UHV chamber is equipped with two electron beam evaporators, a quartz microbalance, an electron beam heater, an ion sputter gun, a mass spectrometer, and an Auger spectrometer (DESA 100 Staib Instruments) arranged in three different levels. Gases are introduced into the chamber via a gas dosing manifold. The sample transfer is achieved by means of a magnetically coupled transfer rod with a Pyrex glass sample car acting also as sample holder in the reaction cell. With this all-glass setup no wires or thermocouples are connected to the sample and background activity is negligible. The main chamber is pumped by a turbomolecular pump, an ion getter pump, and a titanium sublimation pump to a base pressure in the low 10^{-10} mbar range.

A polycrystalline rhodium foil (0.125-mm thickness; purity, 99.9%) and vanadium wire (1-mm ∅; purity, 99.996%) were obtained from Goodfellow. The rhodium foil was cleaned by successive cycles of Ar ion bombardment (500 eV, 0.8-μA sample current), oxidation (2.0×10^{-7} mbar O_2, T up to 1000 K), and annealing in hydrogen (2.0×10^{-7} mbar H_2, T up to 700 K) and in vacuum (at 1000 K) until no impurities were detected by AES. Vanadium oxide overlayers were prepared by reactive evaporation of vanadium from a well-degassed electron beam evaporator in a background pressure of 2.0×10^{-7} mbar oxygen. After deposition the samples were oxidised in 2.0×10^{-7} mbar O_2 at 673 K for 10 min. The deposition rate was monitored by a quartz microbalance. Auger signal vs deposition time plots clearly indicated a layer-by-layer growth of the oxide. The vanadium oxide coverage is always given in monolayer equivalents (MLE) and normalised to a stoichiometry of V_2O_3. One MLE V_2O_3 corresponds to 9.5×10^{14} V atoms/cm^2 (16).

Both sides of the rhodium foil were exposed to the vanadium flux so that the catalyst surface area was relatively high (7.8 cm^2). After preparation the samples were reduced at a given temperature and hydrogen pressure (for 10 min unless stated otherwise). Every preparation step was followed by Auger electron spectroscopy. The Auger spectra were acquired at a 3-keV primary energy in the pulse-counting mode, normalised with respect to the background level at the high-energy side of the respective peak, and differentiated electronically.

After characterisation the samples were transferred to the reactor and exposed to the reactant mixture. The reactants were circulated by means of a metal bellows pump. Samples were taken periodically and analysed by gas chromatography with mass selective detection. Initial reaction rates at 573 K were determined at low conversion from conversion versus time plots. The turnover frequency (TOF) was calculated with respect to the geometric area of the rhodium substrate (7.8 cm^2) assuming a Rh atom density of 1.58×10^{15} atoms/cm^2 (average of close-packed Rh(111) and Rh(100) facets).

After every reaction the sample was oxidised in 2.0×10^{-7} mbar O_2 at 673 K for 10 min in order to remove carbonaceous deposits. Vanadium oxide deposits were removed by cycles of oxidation, Ar ion bombardment, and annealing. Before every step the cleanliness of the sample

was checked by AES and by running a CO hydrogenation reaction under "standard" conditions.

3. RESULTS

3.1. Composition (AES Data)

In a two-dimensional structure the Auger intensities are directly proportional to the surface concentration, so that their changes will reflect changes in the stoichiometry of the overlayer. The surface composition of the sample was monitored by AES after preparation, after subsequent reduction and after every reaction, and the changes of the relevant oxygen and vanadia signals were recorded.

In Figs. 1 and 2 Auger spectra are shown for (Rh + 0.55 MLE V_2O_3) and (Rh + 0.89 MLE V_2O_3), respectively, recorded before and after reduction in 2.0×10^{-7} mbar H_2 for 10 min at different temperatures. (All reduction steps were separated by oxidation in 2.0×10^{-7} mbar O_2 at 673 K for 10 min!)

After vanadium deposition and annealing in 2.0×10^{-7} mbar O_2 at 673 K oxygen remains adsorbed on the bare rhodium patches, as confirmed by a study of the bare rhodium surface. Therefore, the O_{508}/V_{468} Auger signal ratio measured after oxidation, which varies with VO_x coverage, does not provide information about the vanadium oxide stoichiometry. However, oxygen adsorbed on rhodium is easily removed by exposure to hydrogen (2.0×10^{-7} mbar at 373 K). Consistently, the oxygen signal decreases upon exposure to hydrogen at 373 K, while the intensity and peak shapes of the vanadium signals at 468 and 435 eV (V_{468} and V_{435}) are not effected by this reduction. In Fig. 3 the oxygen loss upon reduction at 373 K (determined from the decrease of the two Auger signals, O_{508} and O_{490}) is shown as a function of coverage. In the submonolayer range it decreases with increasing coverage of vanadium oxide, but it is small (~5%) and constant for coverages in excess of 1 MLE. This decrease is therefore due to the removal of adsorbed O from the bare Rh patches, and the remaining oxygen is associated with the vanadium oxide overlayer, which in turn can be characterised by the ratio of vanadium and oxygen signals (O_{508}/V_{468}). After reduction at 373 K O_{508}/V_{468} is 2.9 ± 0.15 in the range of submonolayer coverage, but it is notably smaller for coverages above 1 MLE (e.g., it is 2.5 for Rh + 2.2 MLE V_2O_3). In Fig. 4 the dependence of the Auger signals of Rh, V, and O on the reduction temperature is shown. Raising the reduction temperature in steps from 373 to 573 K does not lead to further changes.

However, increasing the temperature of hydrogen reduction (in 2.0×10^{-7} mbar H_2) above 573 K results in a markedly decreased oxygen signal and concomitantly a decrease of O_{508}/V_{468} (Fig. 4; see also Figs. 1 and 2). In Fig. 3 it is shown that in the submonolayer range O_{508} and O_{490} decrease by about 1/3 between reduction at 373 (or 573) and 673 K. Below 1 MLE coverage the reduction of the signal is constant and must therefore be connected with a change in the VO_x stoichiometry. After reduction at 673 K O_{508}/V_{468} is 1.9 ± 0.1 compared to 2.9 after reduction at or below 573 K.

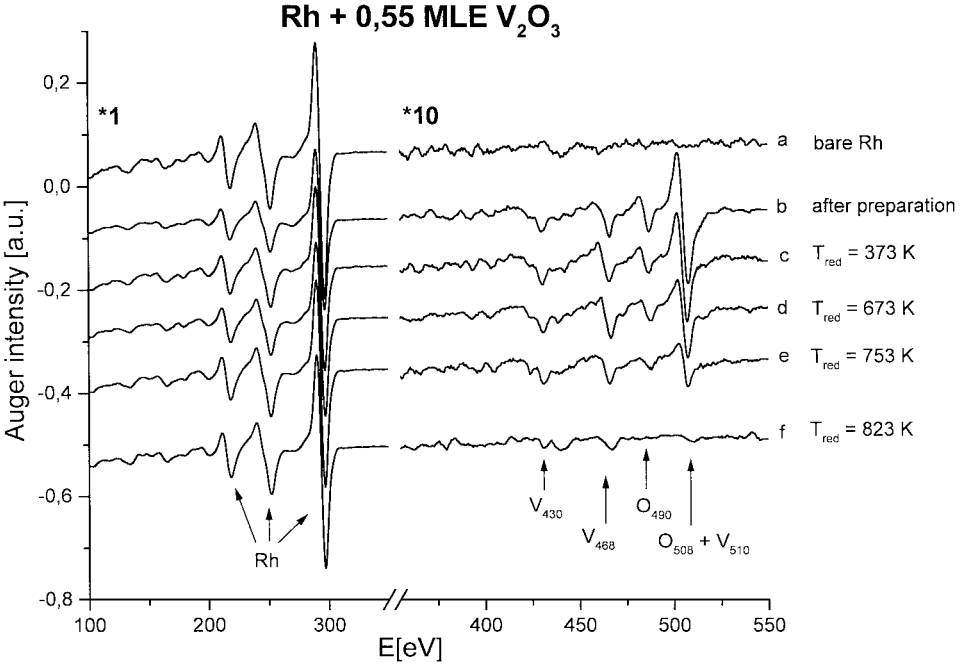

FIG. 1. Auger spectra of the bare Rh surface (a), and of (Rh + 0.55 MLE V_2O_3) immediately after preparation (b) and after reduction at 373 (c), 673 (d), 753 (e), and 823 K (f). Reduction conditions: 2.0×10^{-7} mbar H_2, 10 min; the reduction steps were separated by oxidation in 2.0×10^{-7} mbar O_2 at 673 K for 10 min.

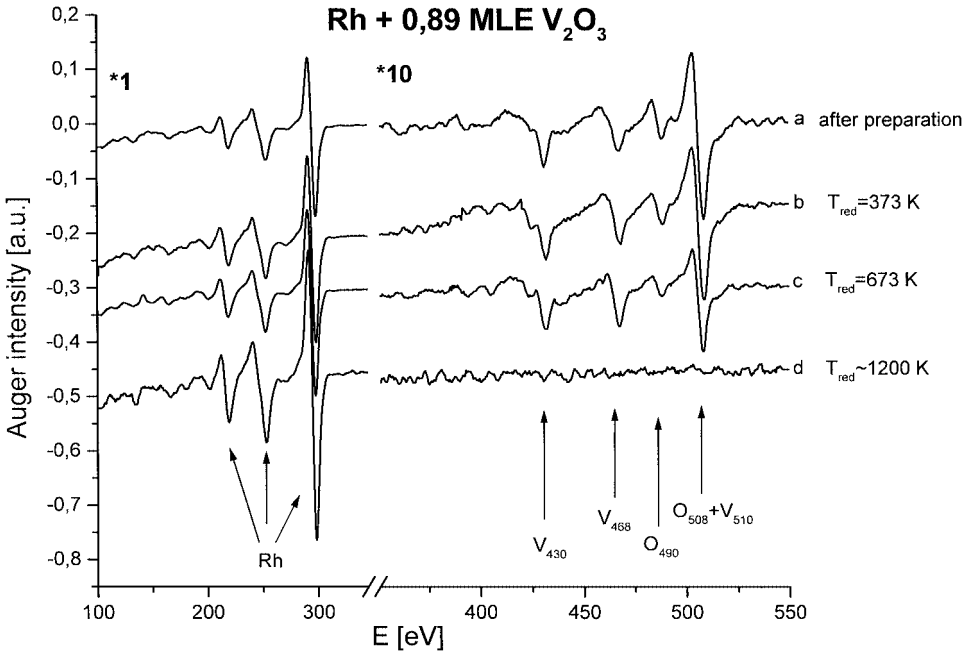

FIG. 2. Auger spectra of (Rh + 0.89 MLE V_2O_3): after preparation (a) and after reduction at 373 (b), 673 (c), and 1200 K (d). Reduction conditions: 2.0×10^{-7} mbar H_2, 10 min (except 1 min in (d)); reduction steps separated by oxidation in 2.0×10^{-7} mbar O_2 at 673 K for 10 min.

At the same time, the ratio of V_{430} to V_{468} has changed from 0.78 ± 0.1 to 1 ± 0.15. In excess of 1 MLE coverage only a slight decrease of the oxygen signals is observed upon reduction at 673 K, and O_{508}/V_{468} is not significantly affected.

The changes described so far are fully reversible by oxidation in 2.0×10^{-7} mbar O_2 at 673 K. Two reductions at 373 K separated by one or more oxidation and reduction cycles (at or below 673 K) result in an identical Auger fingerprint and in the same O_{508} and V_{468} intensities. Furthermore, it is noted that the hydrogen pressure during reduction, either 2.0×10^{-7} or 200 mbar, does not influence the composition of the resulting overlayer.

Thus, it is concluded that under the given conditions submonolayers of vanadium oxide on polycrystalline Rh exist

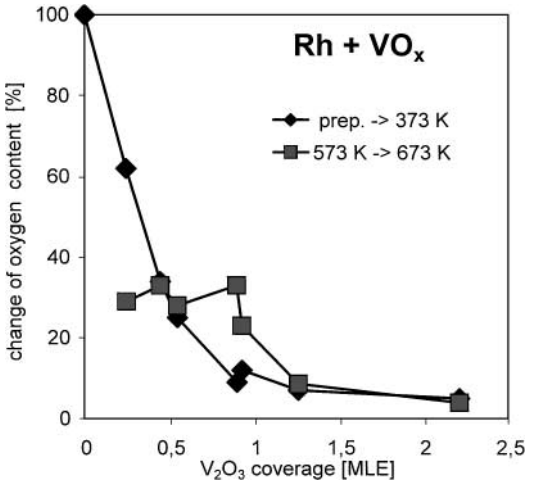

FIG. 3. Oxygen loss of $Rh + VO_x$ between preparation and reduction at 373 K (◆) and between reduction at 373 and 673 K (■) as a function of initial vanadium oxide coverage. Reduction conditions: 2.0×10^{-7} mbar H_2, 10 min, at indicated temperatures. The oxygen loss is determined from the intensity decrease of the O_{490} and O_{508} oxygen Auger signals upon raising the reduction temperature.

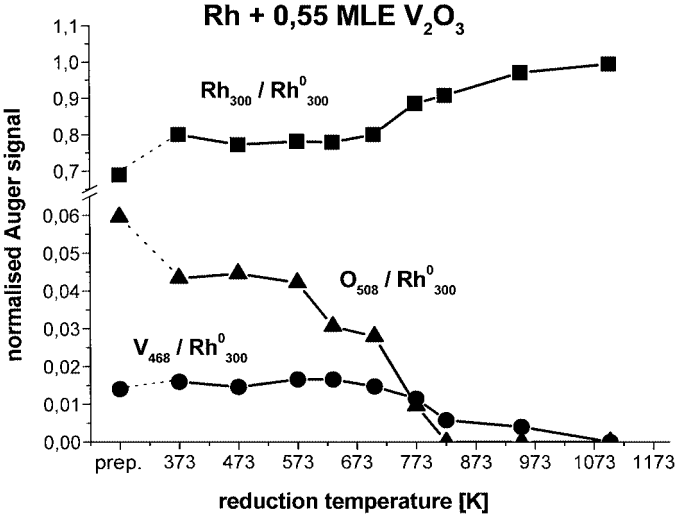

FIG. 4. (Rh + 0.55 MLE V_2O_3): Rh, V, and O Auger signals as a function of the reduction temperature. Intensities are normalised to the main Rh peaks of the bare Rh surface (Rh^0). Reduction conditions: 2.0×10^{-7} mbar H_2, 10 min; reductions separated by oxidation in 2.0×10^{-7} mbar O_2 at 673 K for 10 min.

in two different phases, characterised by $O_{508}/V_{468} = 2.9$ and 1.9, respectively. The transition between these two phases occurs upon reduction in hydrogen between 623 and 673 K. It must be noted that this holds only for the submonolayer regime of vanadium oxide, while for higher coverage the change in the O signals is small, indicating that the VO_x stoichiometry is much less affected.

Raising the reduction temperature above 723 K leads to further significant changes in the Auger spectrum. In this case not only the oxygen signals but also the vanadium signals are altered (Fig. 1). Furthermore, the modifications are no longer completely reversible by cycles of oxidation and reduction.

After reduction above 723 K the oxygen signals O_{508} and O_{490} diminish. On (Rh + 0.55 MLE V_2O_3) oxygen is removed after reduction at 823 K, and V_{430} and V_{468} decrease to about 1/3, as shown, for example, for the sample in Fig. 1f. For a higher coverage (Rh + 0.92 MLE) the changes of V_{468} and O_{508} after reduction at 823 K are shown in Fig. 5. In this case the vanadium and oxygen signals are decreased, but oxygen is not completely removed. A reduction at 873 K is now necessary to remove oxygen entirely from the surface. Concomitantly, V_{468} and V_{430} decrease again to about 1/3 of the initial value. In the intermediate temperature range, from 753 to 773 K, O_{508} (and O_{490}) as well as V_{468} and V_{435} are decreased, but oxygen is still present on the surface and O_{508}/V_{468} is about 1 (Fig. 5).

Since after reduction above 823 K ("high-temperature reduction" (HTR)) no oxygen is detected on the surface,

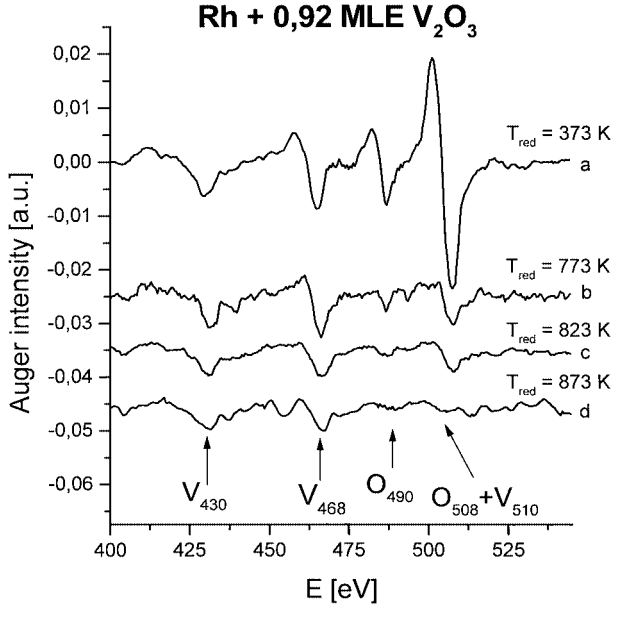

FIG. 5. Auger spectra of (Rh + 0.92 MLE V_2O_3): after reduction at 373 (a), 773 (b), 823 (c), and 873 K (d). Reduction conditions: 2.0×10^{-7} mbar H_2, 10 min; reductions separated by oxidation in 2.0×10^{-7} mbar O_2 at 673 K for 10 min.

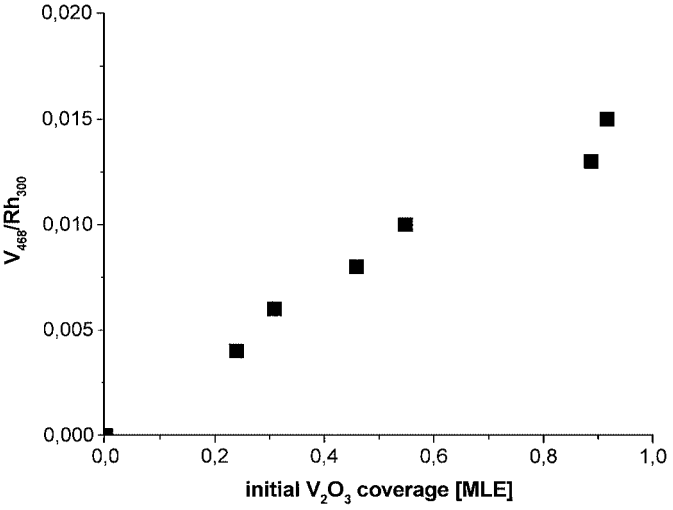

FIG. 6. Surface composition after HTR (2.0×10^{-7} mbar H_2, 823–873 K, 10 min): V_{468}/Rh_{300} Auger signal ratio as a function of initial vanadium oxide coverage.

reduction to metallic vanadium must have occurred. (The apparent $O_{508}/V_{468} < 0.2$ is due to a vanadium peak at 510 eV.) At the same time the intensities of V_{468} and V_{430} are markedly decreased, which can be explained by diffusion of vanadium into near-surface layers.

The ratio V_{468}/Rh_{300} can be used to quantify the vanadium concentration within the information depth of AES (approximately three to five layers). As shown in Fig. 6, V_{468}/Rh_{300} increases with the amount of vanadium oxide initially present on the surface.

After reduction above 1100 K no V_{468} or V_{430} peaks are detected, as shown in Fig. 2, after 1 min reduction of (Rh + 0.89 MLE V_2O_3) at 1200 K. The same is observed upon heating samples with lower coverage above 1100 K. Apparently, the vanadium concentration in the near-surface region has vanished and vanadium is now completely dissolved in the rhodium bulk.

In Fig. 7 it is documented that vanadium segregates from the subsurface region to the surface upon reoxidation (2.0×10^{-7} mbar O_2, 673–873 K, 10–30 min), forming again an oxide overlayer. Auger spectra of (Rh + 0.55 MLE V_2O_3) are shown after two reductions at 373 K (Figs. 7a and 7c) separated by a high-temperature reduction (Fig. 7b) (reduction always after oxidation at 673 K). Oxidising the HTR sample does not reestablish the original vanadium coverage. V_{468} decreases by 10–15% and O_{508}/V_{468} is now 2.7 compared to 2.9 on the original deposit. If we assume that reduction at 373 K will always result in the same vanadium-to-oxygen stoichiometry, part of the vanadium must have remained dissolved in the rhodium bulk after oxidation. However, the resegregation of most of the vanadium upon oxidation, together with the fact that the Auger V_{468} signal is still observed after HTR, supports the conclusion that after reduction, between 723 and 1000 K vanadium remains

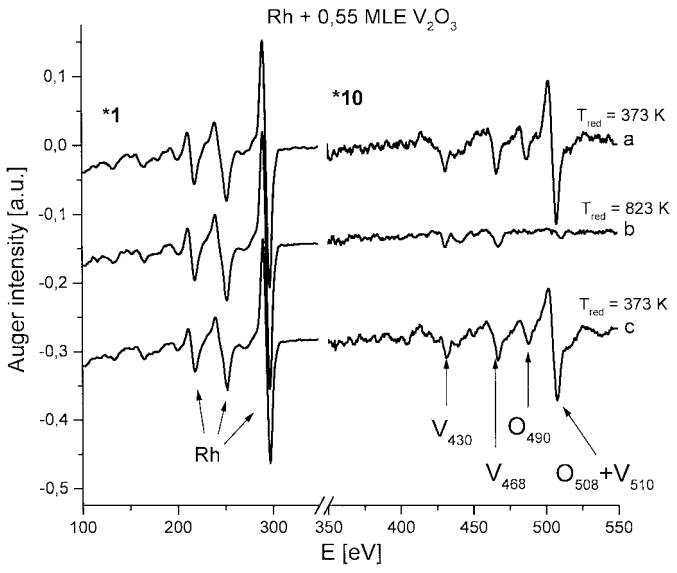

FIG. 7. Auger spectra of (Rh + 0.55 MLE V_2O_3) after sequential reduction at 373 (a), 823 (b), and 373 K (c). Reduction conditions: 2.0×10^{-7} mbar H_2, 10 min; reduction steps separated by oxidation in 2.0×10^{-7} mbar O_2 at 673 K for 10 min.

mainly in the near-surface rhodium layers. After reduction above 1100 K, no vanadium signals are observed, and vanadium does not segregate to the surface even upon prolonged oxidation, which is consistent with complete dissolution in the bulk.

3.2. CO Hydrogenation

The kinetic experiments were performed immediately after reduction in hydrogen at a given temperature and pressure ("prereduction") and after subsequent characterisation by AES. The rate of methane formation from a mixture of 40 mbar CO and 120 mbar H_2 (with He added to 1 bar) on the unpromoted rhodium foil was 0.017 molecules/s·site at 573 K, and no deactivation was observed over long reaction times. Methane is the main product, with a selectivity of more than 96%. The reproducibility of the turnover frequencies (TOFs) is ±4%. The bare Rh surface was exposed to the same gas exposures and treatments as the VO_x-covered samples, but no influence of pretreatment on the activity was observed in this case.

The initial TOF for methane formation on vanadium oxide-promoted rhodium is presented in Fig. 8 as a function of vanadium oxide coverage for prereduction at and below 673 K. Again, the results are shown for the reaction of a stoichiometric CO/H_2 mixture (40 mbar CO and 120 mbar H_2, He added to 1 bar) at 573 K. Each reduction was performed after oxidation in 2.0×10^{-7} mbar O_2 at 673 K for 10 min and immediately prior to the reaction. After prereduction at 373 K the initial rate of methane formation increases with respect to that on the bare surface. Plotting rate vs coverage, we obtain a volcano curve as described by Boffa *et al.* (13). A further rise in the reduction temperature in steps to 573 K does not significantly affect the rates. However, raising it from 573 to 673 K leads to a modest but significant and reproducible rate increase. The relative rate of methane formation for any reduction temperature passes a maximum at a coverage of 0.5 ± 0.05 MLE vanadia, corresponding to a 2.7-fold activity enhancement after reduction at 673 K. Above 0.85 MLE coverage the rate drops below that measured on the bare rhodium surface and the difference between the two prereduction temperatures diminishes. Samples completely vanadium oxide covered are less active than the bare rhodium surface by more than two orders of magnitude.

The selectivity on clean and vanadium oxide-promoted rhodium is summarised in Table 1. With increasing vanadium oxide coverage, the selectivity towards methane decreases from 97 to 55% (on Rh + 0.89 MLE V_2O_3), and more higher alkanes are formed. At the same time the selectivity towards unsaturated products (ethene and propene) increases significantly. At constant coverage, a reduction at 673 K decreases the methane selectivity compared to that after LTR, and increases the ratio of unsaturated to saturated hydrocarbons. The formation of methanol and higher alcohols is well-known under different conditions of temperature and pressure (25, 26) but was not observed under the present experimental conditions.

A further increase in the reduction temperature (HTR, 823–873 K) under 2.0×10^{-7} mbar H_2 leads to another, rather unexpected rate increase. In Fig. 9 the initial TOF after HTR is shown as a function of the initial V_2O_3 coverage. A strong increase is observed for initial coverages up to 0.5 MLE, at which point the TOF levels off, while the rate enhancement is about sixfold compared to the bare

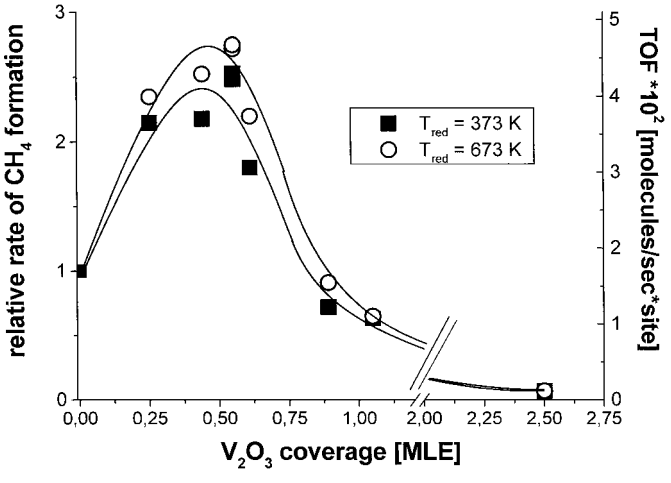

FIG. 8. CO hydrogenation activity after LTR as a function of vanadium oxide coverage. Reaction conditions: 40 mbar CO, 120 mbar H_2, He added to 1000 mbar, $T = 573$ K. Prereduction: 2.0×10^{-7} mbar H_2 at the stated temperature (373 or 673 K), 10 min.

TABLE 1

Selectivity of (Rh + VO_x) after LTR (Measured at Conversions below 2%)[a]

Sample	TOF (1/s · site)	Selectivity (%)				
		Methane	Ethane	Ethene	Propane	Propene
Bare Rh	0.017	97.5	2.5			
0.24 MLE V_2O_3 (T_{red} = 373 K)	0.035	79	9	2	5	5
0.24 MLE V_2O_3 (T_{red} = 673 K)	0.039	68	13	8	4	7
0.55 MLE V_2O_3 (T_{red} = 373 K)	0.042	72	14	3	4	7
0.55 MLE V_2O_3 (T_{red} = 673 K)	0.047	64	12	7	6	11
0.89 MLE V_2O_3 (T_{red} = 373 K)	0.013	55	13	15	2	15
2.2 MLE V_2O_3 (T_{red} = 373 K)	0.0006	40	14	28		18

[a] Reaction conditions: 40 mbar CO, 120 mbar H_2, He added to 1 bar, T = 573 K. Reduction in 2.0×10^{-7} mbar H_2 for 10 min.

Rh surface. The TOFs and selectivities for HTR samples are summarised in Table 2. After high-temperature reduction the selectivity towards methane is between 96 and 93% and does not depend significantly on the initial coverage.

Finally, raising the reduction temperature further, up to ≥1100 K, leads to a strong activity decline (Fig. 9). The selectivity towards methane is >96%, and TOF and selectivity are almost identical to those of the bare rhodium surface.

In Fig. 10 conversion versus time plots are shown for (Rh + 0.55 MLE V_2O_3). The reduction steps (again separated by oxidation at 673 K) are consecutively numbered. In Fig. 10, the hydrogen pressure during reduction was 2.0×10^{-7} mbar in steps 2 and 3, and 200 mbar in steps 4 and 5. For equal reduction temperature the conversion vs time plots are identical, i.e., the hydrogen pressure during prereduction does not influence the activity or the composition of the overlayer, as mentioned before. On the other hand, the activity changes induced by reduction are fully reversible if the reduction temperature is 673 K or below: After two low-temperature reductions (≤573 K) which are separated by one or more cycles of oxidation and reduction at 673 K, identical conversion vs time plots are obtained. This is also demonstrated in Fig. 11, where the *initial* TOFs of three samples with different V_2O_3 coverage are shown after a series of reduction steps (separated by oxidation in 2.0×10^{-7} mbar O_2 at 673 K).

In contrast, if a low-temperature reduction follows a high-temperature reduction (673–873 K, for 10 min) (with oxidation in 2.0×10^{-7} mbar O_2 in between) a higher activity is observed than after low-temperature reduction of an as-prepared VO_x/Rh sample at the same temperature. Thus, after HTR the activity is not reversible by oxidation. In Fig. 10 it is also seen that on the bare rhodium surface the

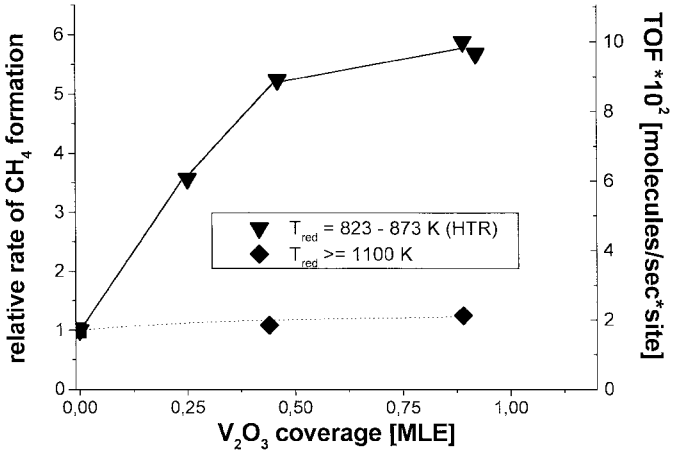

FIG. 9. CO hydrogenation activity after HTR as a function of vanadium oxide coverage. Reaction conditions: 40 mbar CO, 120 mbar H_2, He added to 1000 mbar, T = 573 K. Prereduction: 2.0×10^{-7} mbar H_2 at 823/873 K for 10 min and at 1100 K for 1 min.

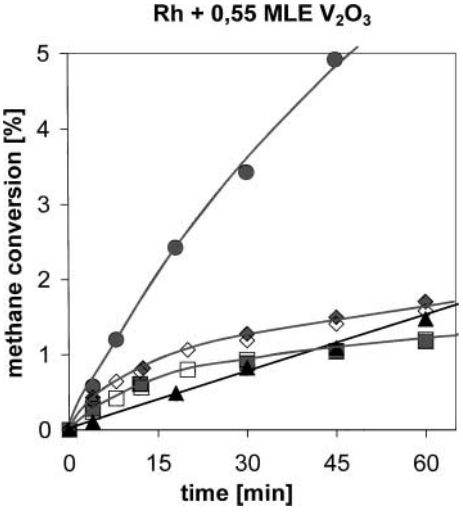

FIG. 10. Conversion vs time plots for (Rh + 0.55 MLE V_2O_3). Reaction conditions: 40 mbar CO, 120 mbar H_2, He added to 1000 mbar, T = 573 K. Prereduction: (□, step 2) 373 and (◇, step 3) 673 K at 2.0×10^{-7} mbar H_2 for 10 min; (■, step 4) 373 and (◆, step 5) 673 K at 200 mbar H_2 for 10 min; and (●, step 6) 823 K at 2.0×10^{-7} mbar H_2 for 10 min. For comparison: (▲, step 1) bare Rh.

TABLE 2

Selectivity of (Rh + VO_x) after HTR (Measured below 3% Conversion)[a]

Sample	TOF (1/s · site)	Selectivity (%)				
		Methane	Ethane	Ethene	Propane	Propene
Bare Rh	0.016	98.5	1.5			
0.24 ML V_2O_3 (T_{red} = 823 K)	0.059	96	3		0.5	0.5
0.55 ML V_2O_3 (T_{red} = 823 K)	0.089	94	3	1	2	
0.92 ML V_2O_3 (T_{red} = 873 K)	0.10	93	6		1	
0.89 ML V_2O_3 (T_{red} = 1200 K)	0.022	95.5	4.5			

[a] Reaction conditions: 40 mbar CO, 120 mbar H_2, He added to 1 bar, T = 573 K. Reduction at indicated T in 2.0×10^{-7} mbar H_2 for 10 min.

methane formation increases linearly with time, while on the oxide-promoted sample a noticeable deactivation is observed with increasing reaction time. On the HTR sample deactivation is much less effective.

Postreaction surface analysis by AES indicates the presence of carbon and small quantities of oxygen-containing species. On the vanadium oxide-promoted surface the "steady state" carbon content is much higher than on the bare surface and it increases with increasing oxide coverage. The reactivity of the deposited carbon was tested by subjecting the sample to 1000 mbar H_2 at 573 K. Only a negligible amount of methane formation was observed and the intensity of the carbon peak decreased by only about 10–20% even after several hours of reaction. Hence, the carbon formed during reaction is not reactive towards hydrogen but is responsible for the observed deactivation by site blocking.

In Fig. 12 postreaction Auger spectra for (Rh + 0.55 MLE V_2O_3) are shown. On the HTR samples carbon formation is generally much less than on oxide-promoted samples. An increased oxygen signal is observed after reaction, but flashing the samples briefly to 623 K removes adsorbed CO and/or other adsorbed oxygen-containing species and decreases the oxygen signal to the level measured on bare rhodium under identical conditions. Thus there is no indication for the oxidation of vanadium to vanadium oxide or the formation of vanadium carbide during reaction. As mentioned before, the above results were all obtained from a CO : H_2 mixture of stoichiometry of 1 : 3 at 573 K (40 mbar CO and 120 mbar H_2 and with He added to 1 bar total pressure). Raising the hydrogen partial pressure to 400 and 1000 mbar at constant CO pressure and coverage leads to an increase in the promotional effect. In agreement with previous work (13, 15) a reaction order of about 1 with

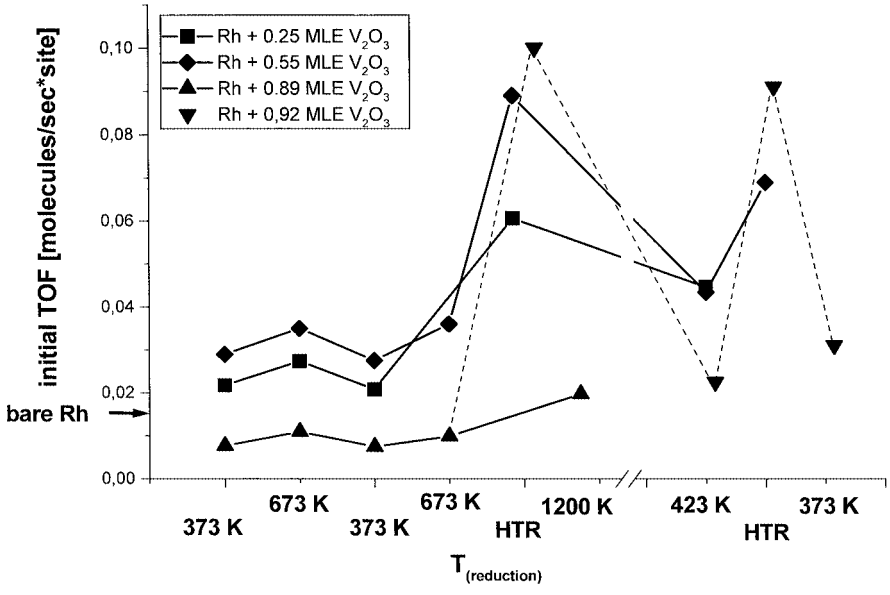

FIG. 11. Initial turnover frequency during a sequence of reduction steps. Reaction conditions: 40 mbar CO, 120 mbar H_2, He added to 1000 mbar, T = 573 K. Prereduction: 2.0×10^{-7} mbar H_2 at the stated temperature, 10 min; reductions separated by oxidation at 673 K, 2.0×10^{-7} mbar O_2 for 10 min.

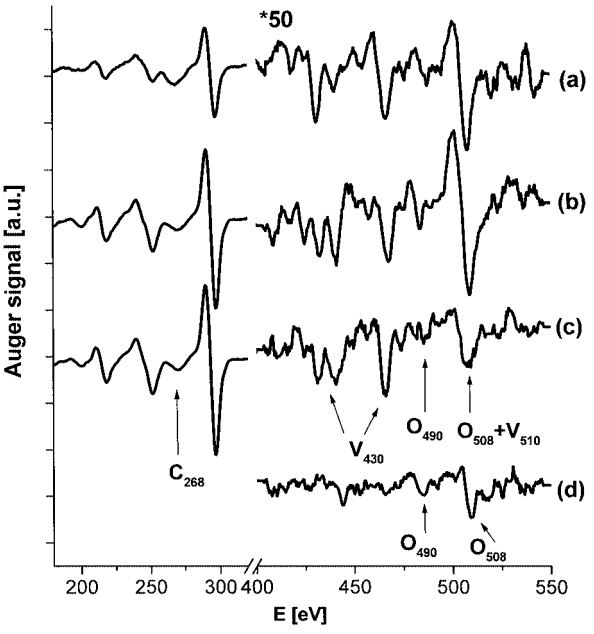

FIG. 12. Postreaction spectra of (Rh + 0.55 MLE V_2O_3): reaction after LTR (673 K) (a), reaction after HTR (823 K) (b), and reaction after HTR followed by flashing to 623 K (c). For comparison: bare Rh surface after reaction and flashing to 623 K (d).

respect to hydrogen and a slightly negative order with respect to CO were determined.

4. DISCUSSION

4.1. Structure and Composition

The preparation procedure applied in this study is similar to that used by Boffa *et al.* (13) for the preparation VO_x on polycrystalline rhodium and to that by Hartmann *et al.* (15) for the preparation of VO_x on Rh(111). They both observed two-dimensional island growth and assigned a valence state 3^+ to vanadium in the as-grown oxide overlayer on the basis of core level shifts in XPS, corresponding to a "V_2O_3"-type stoichiometry. Depending on the reduction temperature they found a changing proportion of V^{3+} to V^{2+} ions in the oxide overlayer, indicating a reduction of the initial V_2O_3 oxide. On Pd(111) Surnev and coworkers (16–19) observed various surface structures with increasing coverage, and with three-dimensional growth starting only just below monolayer oxide coverage. In the submonolayer range VO_x grows in two dimensions either along steps of the Pd surface or as circular islands on the terraces. Upon annealing the layers become very mobile and may change from more open to more closed surface structures. The stoichiometry of the low-coverage 2D phases is usually V^{3+}, but V^{4+} may also be present depending on the preparation conditions. Ab initio density functional theory calculations (18) confirmed that a surface V_2O_3 layer is the energetically most stable configuration. Upon heating in vacuum above 673 K the oxide decomposes and is converted in island structures of a V/Pd subsurface alloy with a palladium-terminated surface, without ever adopting the valence state V^{2+} (18, 19).

In our experiments the plots of the respective Auger intensities vs the amount of deposited vanadium (determined with the quartz microbalance) exhibit linear segments with slope changes agreeing with two-dimensional island growth in the submonolayer range. Upon deposition of one nominal monolayer V_2O_3 Rh_{300} decreases linearly to 0.65 of its initial value. We can assume that on the polycrystalline Rh surface preferential growth will occur along step edges, but also along the grain boundaries.

It is convenient to separate two different situations—vanadium oxide overlayers after low-temperature reduction (LTR, $\leq$673 K) and vanadium metal in the surface region after HTR at 823 K and above. (The status of the surface after reduction between 673 and 823 K is not reproducible and mainly determined by the duration of the reduction.)

After reduction at or below 673 K vanadium oxide overlayers are stable and were identified in two different compositions:

- Reduction between 373 and 573 K leads to a composition characterised by $O_{508}/V_{468} = 2.9 \pm 0.15$ (cf., phase I).
- Reduction between 623 and 723 K leads to an oxide overlayer with $O_{508}/V_{468} = 1.9 \pm 0.1$ (phase II).

In principle this is consistent with the findings of Boffa *et al.* (13) and Hartmann and Knözinger (15), who measured a changing proportion of V^{3+} to V^{2+} ions on the surface depending on the reduction conditions. However, the fact that the calculations by Kresse and coworkers (19) exclude the existence of a (thermodynamically) stable VO phase on Pd(111), and possibly also on a Rh(111) surface, has led us to consider other possible stoichiometries for phases I and II. In fact, a recent STM investigation by Netzer and coworkers (23) revealed that vanadia adlayers on Rh(111) may adopt a variety of as yet undetermined surface structures under different preparation conditions.

In an earlier study Szalkowski and Somorjai (27, 28) investigated oxide powder samples of different stoichiometry and related the Auger intensities to the oxidation state of vanadium. They measured the ratio O_{508}/V_{468}, but also the ratio of the vanadium valence band transition ($V_{LMV} = V_{468}$) to the vanadium inner shell transition ($V_{LMM} = V_{430}$). V_{468}/V_{430} increases with decreasing oxidation state due to the different occupation of the vanadium valence band. Using Szalkowski's findings and the relative sensitivity factors tabulated in the *Handbook of Auger Electron Spectroscopy* (29) we obtain a formal stoichiometry of V_3O_7 for phase I and of V_2O_3 for phase II. However, for many reasons, such as the different electron escape depths, different

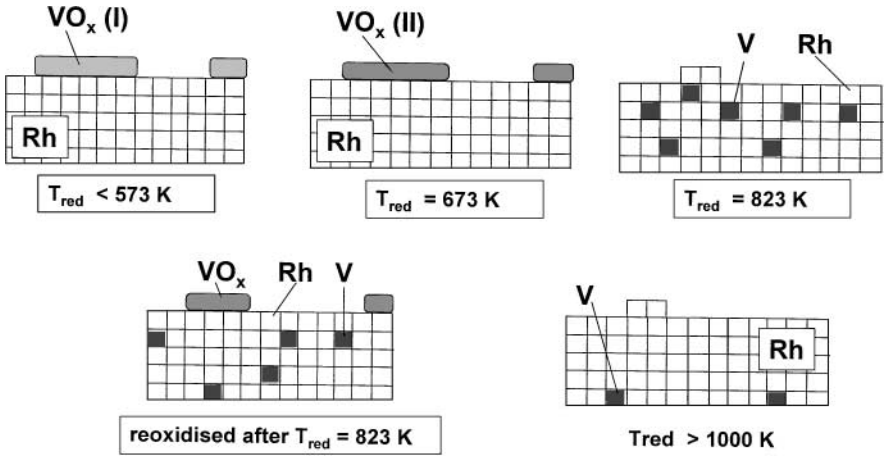

FIG. 13. Scheme of the change of the surface composition of Rh/VO_x with increasing reduction temperature.

backscattering factors, and adsorbate–substrate interactions, Auger data measured on bulk samples and on thin films are not readily comparable even if the same experimental setup is used. On the other hand, structures which are thermodynamically unfavourable on a single crystal surface may be kinetically stable on the polycrystalline Rh surface. Hence, at present we must conclude that the initial stoichiometry is between V_3O_7 and V_2O_3 (phase I) and that reduction at 673 K leads to a kinetically stable phase II of a formal composition between V_2O_3 and VO. Upon transition between the two phases no change of the vanadium concentration on the surface is observed, and the position of the activity maximum with respect to the nominal (V_2O_3) coverage is not altered.

A high-temperature hydrogen treatment (823–873 K) leads to a complete reduction of the vanadium oxide to metallic vanadium. The V_{468} signal is markedly attenuated and hence the vanadium concentration on the surface is decreased (see, e.g., Fig. 4). Metallic vanadium and rhodium are well miscible and several alloys of V and Rh are known. In separate experiments (30) it could be shown that vanadium metal overlayers on rhodium exchange with the rhodium substrate upon annealing in UHV above 700 K. Thus, after reduction of the oxide at elevated temperature, the resulting metallic vanadium diffuses into the bulk. The fact that V_{468} and V_{430} are still detected by AES indicates that it remains in the near-surface region. The concentration of vanadium in the near-surface region can be quantified by the V_{468}/Rh_{300} signal ratio which increases almost linearly with increasing initial vanadium oxide coverage upon reduction between 823 and 873 K (Fig. 6). On the Rh(111) surface a rhodium–vanadium subsurface alloy of defined stoichiometry has been recently characterised by STM (22). Its rhodium-terminated surface contains a high density of atomic steps. If the reduction temperature is increased above 1000 K, no vanadium is present in the near-surface region, but it is dissolved in the rhodium bulk. A schematic presentation of the surface composition as a function of reduction temperature is given in Fig. 13.

4.2. Catalytic Activity

This section relates the measured catalytic activity to the composition and structure of the sample before and after reaction.

From Fig. 8, where the activity is shown as a function of oxide coverage, we see that the maximum rate enhancement is reached near 0.5-ML coverage, as in the earlier observations (13). In contrast, thick layers of vanadium oxide are about two orders of magnitude less active and therefore vanadium oxide alone cannot be responsible for the activity enhancement. Hence, upon reduction between 373 and 573 K the reaction will occur at the perimeter of vanadium oxide islands. These islands (phase I) have a defined structure, probably similar to that observed on Pd(111). With increasing reduction temperature they loose oxygen (Fig. 5) and are transformed to phase II. The kinetic experiments reveal a small but reproducible enhancement of the initial activity upon raising the reduction temperature from 573 to 673 K (Fig. 8), which is clearly related to the changing vanadium oxide stoichiometry.

As mentioned before, promotion of the CO hydrogenation by reducible oxides has been observed long ago on different noble metals (e.g., 8, 31, 32). Burch and Flambard (33, 34) were among the first to propose that the interface between metal and oxide provides highly active sites and that the activation of adsorbed CO occurs via an interaction of the oxygen end with cationic centres or oxygen vacancies present at the interface. On regular catalysts the study of the effect of metal–oxide interactions is impeded by the difficulties in controlling and defining the structure and morphology. On metal surfaces decorated by oxide overlayers Boffa *et al.* (14) demonstrated that the extent of promotion by reducible oxides is related to the reducibility and the

Lewis acidity of the oxide. The idea of describing the interaction between CO and reduced oxides as Lewis acid–base complexes was first suggested by Sachtler *et al.* (35, 36).

The postreaction analysis by AES reveals that the amount of carbon is significantly greater on vanadium oxide-covered rhodium than on the bare rhodium surface. The amount of carbon depends on the oxide coverage and on the hydrogen excess in the reactant gas. On the bare rhodium surface the unreactive carbon species formed after long reaction times is clearly responsible for catalyst deactivation. On the vanadium oxide-promoted catalyst the rate of carbon formation is higher and deactivation therefore much faster and more pronounced. Therefore, if the CO/hydrogen ratio is relatively high (e.g., 1 : 3, corresponding to the stoichiometry of the reaction) the promotion is mainly an *initial* effect. Vanadium oxide at the interface promotes the dissociation of the C–O bond; thus the rates of both carbon formation and carbon hydrogenation are increased. In the steady state the vanadium oxide-covered samples are generally less active because the carbon deposits block the surface.

The postreaction spectra also indicate that the oxygen-to-vanadium stoichiometry has decreased during the reaction, almost independently of the reaction conditions. A similar decrease has been observed upon treatment of the sample in 40 mbar CO at reaction temperature. The reducing potential of CO is high enough to partially reduce the vanadium oxide. After a reaction, or after a reduction in CO, the ratio of O_{508}/V_{468} decreases to 1.65 ± 0.15, fairly independent of its initial value after prereduction. (A more detailed analysis of this surface is impeded because the carbon deposition during reduction affects the overall Auger intensities and does not allow comparison with the clean sample). This means that the initial state (phase I or II) influences mainly the *initial* activity but not the steady state. At a lower CO/hydrogen ratio the original reduction state can be maintained over longer reaction times and deactivation by carbon is considerably reduced.

As is also well-known from bulk catalysts (25, 26) the promotion by vanadium oxide results in an increased selectivity of rhodium towards longer-chain hydrocarbons. This is also reflected in the present results. Moreover, the selectivity is determined by the choice of the prereduction temperature. Reduction at 673 K decreases the selectivity to methane and increases the ratio of unsaturated to saturated hydrocarbons. Higher pressures, lower temperature, and/or a lower H_2/CO ratio would have to be applied in order to produce appreciable amounts of oxygenates (25, 26).

A completely different catalytic behaviour is observed when after high-temperature reduction a rhodium-terminated surface is formed with vanadium occupying subsurface layers. If two samples of equal initial coverage are compared after LTR and HTR, the HTR sample shows higher activity, less deactivation, and less selectivity towards higher alkanes. The TOF increases initially with coverage, as after LTR, but it levels off above about 0.5 MLE (Fig. 9). On HTR samples methane is the main product (93–96%), occurring in amounts similar to that measured on the bare rhodium surface (Table 2). Since V_{468}/Rh_{300} also increases with initial coverage it is concluded that the extent of promotion is related to the concentration of vanadium in the subsurface region. Postreaction Auger spectra show that segregation of vanadium to the surface and oxidation of vanadium to VO_x do not occur upon reaction, at least not in measurable amounts. Therefore, the promoting effect observed after HTR cannot be attributed to the presence of vanadium oxide. However, a synergistic effect of subsurface vanadium and small patches of vanadium oxide, which may be produced during reaction, cannot be completely excluded.

Upon oxidation of HTR samples at 673 K vanadium segregates back to the surface and forms vanadium oxide (Fig. 7). V_{468} is reduced by 10–15% with respect to the original LTR sample. Therefore, the segregation is not quantitative and the original vanadium oxide coverage is not regained. Nevertheless, although the oxide coverage is reduced, the catalytic activity is still higher than on the original VO_x-covered surface independent of the initial coverage (Fig. 11). Furthermore, these catalysts are less susceptible to deactivation and exhibit a higher selectivity towards methane compared to the original LTR catalyst. The O_{508}/V_{468} ratio after HTR–LTR is also smaller than on the original LTR sample, e.g., 2.7 vs 2.9 for (Rh + 0.55 MLE V_2O_3). If we assume that the vanadium oxide overlayer has the same stoichiometry in both cases (LTR and HTR–LTR), the incomplete surface segregation indicates that some vanadium remains in near-surface layers under the stated conditions. The most likely structure of the resulting surface is thus a vanadium oxide overlayer on top of a V/Rh subsurface alloy (Fig. 13). Such a mixed surface composition may well explain why the catalytic properties (activity, selectivity, deactivation) of these surfaces are between those of the HTR and the LTR samples. It seems that in this case the promotion is a synergistic or at least a combined effect of vanadium oxide and of subsurface vanadium.

Postreaction Auger spectra (Fig. 12) show that the carbon content of the HTR samples after reaction is very low and comparable to that of the bare rhodium surface, i.e., much smaller than on vanadium oxide-covered surfaces. In connection with the low carbon level the deactivation is almost negligible.

For a comparison, rhodium surfaces with top layers of metallic vanadium were also prepared by deposition of submonolayers of vanadium at room temperature, and their catalytic activity in the CO hydrogenation was tested. At the start of the reaction a slight promotion was observed but deactivation occurred very rapidly. Strong carbon and

oxygen Auger signals indicate that the vanadium overlayer was converted to vanadium oxide and/or carbide during the reaction. This means that on-top vanadium has completely different catalytic properties and cannot be responsible for the observed promotion.

The origin of the promotion is still a matter of debate. In the case of VO_x overlayers it is very likely that the dissociation of CO remains the rate-limiting step, and that this step is favoured by the presence of low-valent vanadium species and/or oxygen vacancies at the metal–oxide boundary. If the dissociation probability is much enhanced it is conceivable that the rate-limiting step shifts to CH_x hydrogenation (11), but under the present experimental conditions no indication of such a shift (e.g., a change in the reaction order, etc.) was observed. On the other hand, other mechanisms, such as electrostatic activation of the molecule centre (37), cannot be excluded as long as an experimental proof of CO predissociation is lacking.

On the subsurface alloy CO is more weakly bound than on clean Rh (20). Hence CO dissociation will not be enhanced on a flat surface which excludes this as a reason for the observed promotion of CO hydrogenation by subsurface vanadium. Nevertheless, the drastic increase in hydrogenation rates may be explained by a combination of CO dissociation on step edges and increased hydrogen coverage on the terraces: As observed by STM on the V subsurface alloys of Pd (21) as well as of Rh (22) the alloy surfaces are never flat on an atomic scale but contain a high density of irregular steps and other defects which arise during their formation. It is very likely that CO dissociation, and therefore also CO hydrogenation, are enhanced along these step edges. On the other hand, the lower binding energy leads to a lower surface concentration of CO on the terraces. Reduced site blocking by CO, in turn, will increase the relative surface concentration of hydrogen and hence result in a higher reaction rate in the frame of a Langmuir–Hinshelwood mechanism. To prove this hypothesis a more detailed investigation of the alloy surface structure and morphology will of course be necessary.

5. CONCLUSIONS

Vanadia adlayers on a Rh surface promote the hydrogenation of CO. In the present study this promotion was investigated, with emphasis on the effect of the oxidation state of vanadium on the catalytic activity. The initial reaction rates depend strongly on the temperature of hydrogen reduction. The observed increase of the reaction rate by reduction up to 673 K can be correlated to the existence of two adlayer phases of different composition. CO dissociation is enhanced at the perimeter sites of the VO_x islands, leading to enhanced hydrogenation rates but also to enhanced deactivation. If the reduction temperature is raised above 723 K, VO_x is reduced to metallic V and is partially dissolved in the bulk, resulting in a V/Rh subsurface alloy with a Rh-terminated surface. This surface is particularly active and less susceptible to deactivation by carbon deposition.

ACKNOWLEDGMENTS

This work was supported by the Austrian Science Fund within the Joint Research Project "Gas Surface Interactions" (S 8105). We also thank the members of the research project for their continuous cooperation.

REFERENCES

1. Tauster, S. J., Fung, S. C., and Garten, R. L., *J. Am. Chem. Soc.* **100**, 170 (1978).
2. Singh, A. K., Pande, N. K., and Bell, A. T., *J. Catal.* **94**, 422 (1985).
3. Sadeghi, H. R., and Henrich, V. E., *J. Catal.* **87**, 279 (1984).
4. Braunschweig, E. J., Logan, A. D., Datye, A. K., and Smith, D. J., *J. Catal*. **118**, 227 (1989).
5. Bernal, S., Botana, F. J., Calvino, J. J., Lopez, C., Perez-Omil, J. A., and Rodríguez-Izquierdo, J. M., *J. Chem. Soc. Faraday Trans.* **92**, 2799 (1996).
6. Pesty, F., Steinrück, H. P., and Madey, T. E., *Surf. Sci.* **339**, 83 (1995).
7. Bernal, S., Calvino, J. J., Cauqui, M. A., Cifredo, G. A., Jobacho, A., and Rodríguez-Izquierdo, J. M., *Appl. Catal. A* **99**, 1 (1993).
8. Vannice, M. A., *J. Catal.* **37**, 449 (1975).
9. Demmin, R. A., and Gorte, R. J., *J. Catal.* **105**, 373 (1987).
10. Levin, M. E., Salmeron, M., Bell, A. T., and Somorjai, G. A., *J. Catal.* **106**, 401 (1987).
11. Williams, K. J., Boffa, A. B., Lahtinen, J., Salmeron, M., Bell, A. T., and Somorjai, G. A., *Catal. Lett.* **5**, 385 (1990).
12. Williams, K. J., Boffa, A. B., Salmeron, M., Bell, A. T., and Somorjai, G. A., *Catal. Lett.* **9**, 41 (1991).
13. Boffa, A. B., Bell, A. T., and Somorjai, G. A., *J. Catal.* **139**, 602 (1993).
14. Boffa, A. B., Lin, C., Bell, A. T., and Somorjai, G. A., *Catal. Lett.* **27**, 243 (1994).
15. Hartmann, Th., and Knözinger, H., *Z. Phys. Chem.* **197**, 113 (1996).
16. Leisenberger, F. P., Surnev, S., Vitali, L., Ramsey, M. G., and Netzer, F. P., *J. Vac. Sci. Technol. A* **17**, 1743 (1999).
17. Leisenberger, F. P., Surnev, S., Koller, G., Ramsey, M. G., and Netzer, F. P., *Surf. Sci.* **444**, 211 (1999).
18. Surnev, S., Vitali, L., Ramsey, M. G., Netzer, F. P., Kresse, G., and Hafner, J., *Phys. Rev. B* **61**, 13495 (2000).
19. Surnev, S., Kresse, G., Ramsey, M. G., and Netzer, F. P., *Phys. Rev. Lett.* **87**, 086102 (2001) .
20. Hayek, K., Jenewein, B., Klötzer, B., and Reichl, W., *Top. Catal.* **14**, 25 (2001).
21. Konvicka, C., Jeanvoine, Y., Lundgren, E., Kresse, G., Schmid, M., Hafner, J., and Varga, P., *Surf. Sci.* **463**, 199 (2000).
22. Konvicka, C., and Varga, P., *et al.*, manuscript in preparation.
23. Schoiswohl, H., Surnev, S., and Netzer, F. P., *et al.*, manuscript in preparation.
24. Reichl, W., Rosina, G., Rupprechter, G., Zimmermann, C., and Hayek, K., *Rev. Sci. Instrum.* **71**, 1495 (2000).
25. Van der Lee, G., Bastein, A. G. T. M., van den Bogert, J., Schuller, B., Luo, H. Y., and Ponec, V., *J. Chem. Soc. Faraday Trans. 1* **83**, 2103 (1987).
26. Beutel, T., Alekseev, O. S., Ryndin, Yu. A., Likholobov, V. A., and Knözinger, H., *J. Catal.* **169**, 132 (1997).

27. Szalkowski, F. J., and Somorjai, G. A., *J. Chem. Phys.* **61**, 2064 (1974).
28. Szalkowski, F. J., and Somorjai, G. A., *J. Chem. Phys.* **56**, 6097 (1972).
29. Davis, L. E., MacDonald, N. C., Palmberg, P. W., Riach, G. E., and Weber, R. E., Eds., "Handbook of Auger Electron Spectroscopy." Physical Electronic Ind., Eden Prairie, MN, 1978.
30. Reichl, W., and Hayek, K., manuscript in preparation.
31. Pande, N. K., and Bell, A. T., *J. Catal.* **98**, 7 (1986).
32. Haller, G. L., and Resasco, D. E., *Adv. Catal.* **36**, 173 (1989).
33. Burch, R., and Flambard, A. R., *J. Catal.* **78**, 389 (1982).
34. Burch, R., and Flambard, A. R., *J. Catal.* **86**, 384 (1982).
35. Sachtler, W. M. H., and Ichikawa, M., *J. Phys. Chem.* **90**, 4752 (1986).
36. Sachtler, W. M. H., Shriver, D. F., Hollenberg, W. B., and Lang, A. F., *J. Catal.* **92**, 429 (1985).
37. Bonačić-Koutecký, V., Koutecký, J., Fantucci, P., and Ponec, V., *J. Catal.* **111**, 409 (1988).